Ultrasonic welding of carbon/epoxy and carbon/PEEK composites through a PEI thermoplastic coupling layer

Villegas, Irene Fernandez; van Moorleghem, Regis

DOI
10.1016/j.compositesa.2018.02.022

Publication date
2018

Document Version
Accepted author manuscript

Published in
Composites Part A: Applied Science and Manufacturing

Citation (APA)
Villegas, I. F., & van Moorleghem, R. (2018). Ultrasonic welding of carbon/epoxy and carbon/PEEK composites through a PEI thermoplastic coupling layer. *Composites Part A: Applied Science and Manufacturing*, *109*, 75-83. https://doi.org/10.1016/j.compositesa.2018.02.022

Ultrasonic welding of carbon/epoxy and carbon/PEEK composites through a PEI thermoplastic coupling layer

Irene F. Villegas[1,2] and Regis van Moorleghem[1]

[1]Aerospace Structures and Materials Department, Faculty of Aerospace Engineering

Delft University of Technology

Kluyverweg 1, 2629HS, Delft, The Netherlands

[2] Corresponding author: Irene Fernandez Villegas, I.FernandezVillegas@tudelft.nl

Abstract

This paper investigates welding of carbon/epoxy and carbon/PEEK composites using the following procedure. Firstly, the carbon/epoxy composite was made "weldable" through a very thin PEI thermoplastic film co-cured on its surface. During the curing cycle, the PEI resin and the components of the epoxy resin system partially diffused into each other generating a gradient interphase between the original epoxy and PEI resins. Subsequently, the carbon/PEEK composite adherend was welded onto the PEI-rich surface of the weldable carbon/epoxy adherend, exploiting the total miscibility between PEI and PEEK. Thermal degradation of the carbon/epoxy adherend during the welding process was avoided via the ultra-short heating times enabled by the ultrasonic welding technology. In this research, mechanical testing was used to evaluate the weld strength relative to reference joints. Additionally, cross-section scanning electron microscopy was used to assess the morphology of the PEI/epoxy interphase before and after the welding process.

Keywords: A.Thermoplastic resin, A; Thermosetting resin; A. Polymer-matrix composites (PMCs); E. Joints/joining

1. Introduction

Owing to their cost-effectiveness in manufacturing, thermoplastic composites (TPCs) are increasingly found in engineering applications. An example of this are the thousands of press-formed TPC clips (mostly made out of carbon fibre reinforced poly-ether-ether-ketone, carbon/PEEK) used as structural connections in the fuselage of the modern thermoset composite (TSC) passenger aircraft (mostly made out of carbon/epoxy), such as Airbus A350 and Boeing 787. Currently, dissimilar composite parts are assembled through mechanical fastening, which is the preferred assembling method for aircraft metallic structures. Mechanical fastening is however not a composite-friendly joining technique owing to stress concentrations and the necessity to drill holes, which cut through the fibre reinforcement, for fastener installation. TPCs are well known for their ability to be welded or fusion bonded in a fast and energy efficient manner and several thermoplastic composite welding processes have already been developed to a high level of maturity [1,2]. An interesting question is whether it is possible to also apply welding to dissimilar composite, i.e. TPC and thermoset composite (TSC) combinations, as a composite-friendly alternative to current assembling procedures.

In parallel with the increasing use of thermoplastic composites, the effort to develop welding strategies for dissimilar composites has grown in the last years. As a first step to welding TSCs and TPCs, the TSC adherend needs to be made “weldable”. Typically, a weldable TSC has a thermoplastic-rich layer, referred to as thermoplastic “coupling layer” hereafter, on one of its surfaces. The thermoplastic coupling layer is added to the un-cured TSC (or to the dry reinforcement in the case of liquid moulding processes) and, subsequently, the TSC-coupling layer stack is subjected to a curing process. Even though only the TS resin undergoes a curing reaction, that process is referred to as “co-curing” in the literature [3]. For consistency with already published research this term is also used in the present paper.

Several solutions have been shown in the literature to achieve a strong connection between the thermoplastic coupling layer and the TSC during the co-curing process [3,4,5, 6,7]. Particularly

relevant to the research presented in the present paper is a solution that entails using a thermoplastic material for the coupling layer which is compatible with the thermoset resin in the TSC laminate [4]. Mostly from the research and development on toughened thermoset systems, some thermoplastic and thermoset combinations are known to show some degree of miscibility or, in other words, to be compatible with each other. Some examples of thermoplastic resins reported to be compatible with common epoxy systems are polyetherimide (PEI), polysulfone (PSU) and polyethersulfone (PES) [5,8,9], all of them with an amorphous nature. During the curing process, reactive thermoset monomers in a liquid state diffuse into the compatible glassy thermoplastic polymer and partially dissolve it. The dissolved thermoplastic polymer chains are able then to diffuse into the liquid thermoset resin. Once the thermoset resin reaches its gel point, this interdiffusion process stops resulting in a thermoset-thermoplastic micron-size gradient interphase with a gradient composition between the pristine thermoset and the thermoplastic resin systems [8]. In those cases where there is limited solubility between the thermoplastic and the cured thermoset polymers, for instance PEI and PSU in combination with common epoxy systems [5], phase separation occurs upon gelation of the thermoset resin. This results in a distinct gradient morphology within the gradient interphase which, according to literature, can be resolved through optical microscopy [5], atomic force microscopy [5,8,9], scanning electron microscopy [8] and transmission electron microscopy [8]. In other cases, such as PES and some common epoxy systems [5], increased solubility results in no phase separation and hence a gradient interphase composed of a single-phase polymer blend with interdiffused polymer networks [5]. When producing weldable TSCs, the connection of the TSC with the thermoplastic coupling layer through such a gradient interphase is of great interest since it can be detected and characterized and it is believed to be strong and durable [4]. In the case of systems with enhanced solubility the strength of the interphase results from bonding of the interdiffused polymer chains at a molecular level. In the case of systems with limited solubility the strength of the interphase results from bonding of the different phases in

the gradient morphology. On the downside, using a compatible coupling layer imposes great limitations to the dissimilar composite combinations it can be used for.

Alternative solutions to connect a wider range of TSCs and thermoplastic coupling layers can also be found in literature. One of them uses a coupling layer consisting of a fibre fabric reinforcement which is impregnated only half way through with the thermoplastic resin. During co-curing with the TSC laminate, the thermoset resin impregnates the other half of the fabric reinforcement in the coupling layer [6]. Another solution entails treating the thermoplastic coupling layer prior to the co-curing process to improve its adhesion with the thermoset resin in the TSC. Ultraviolet-ozone (UV-O_3) treatment of the thermoplastic coupling layer has shown promising results in this area [7,10]. Alternatively, the surface of the cured TSC laminate can be laser treated to generate a certain texture that will be filled out by thermoplastic resin during the welding process resulting in mechanical interlocking [11]. Note that this last solution does not make use of a coupling layer, but implies direct welding of a TPC on the treated surface of the TSC. Understandably, some of the main points of concern in these solutions are the strength and durability of the TS-TP connection.

The second step in welding TSCs and TPCs is the actual welding process. In the most common case of a weldable TSC adherend provided with a TP coupling layer, the matrix of the TPC adherend will ideally be of the same nature as the coupling layer. During the welding process, heat is applied to the coupling layer-TPC interface, i.e. the welding interface, while the adherends are pressed against each other under a certain welding pressure. Under these conditions, intimate contact at the welding interface is achieved first. Secondly, polymer chain interdiffusion across the interface, i.e. autohesion, occurs provided that the temperature at the welding interface is above the glass transition temperature (for amorphous TP polymers) or the melting temperature (for semi-crystalline TP polymers) of the TP polymer. Finally, the welded interface is cooled down and consolidated under pressure [12]. The performance of such a TPC-TSC welded joint depends on: (i)

the degree of autohesion reached at the welding interface during the welding process; (ii) the connection generated between the coupling layer and the TSC adherend in the co-curing process; and (iii) the properties of the coupling layer and of the adherends themselves. Consequently, high-performance welded joints between high-performance TPC and TSC materials, as it is the focus of the current paper, will benefit from the use of high-performance coupling layers strongly connected to the TSC adherend (co-curing process) and to the TPC adherend (welding process). High-performance thermoplastic polymers however feature welding temperatures that are well above the curing temperature of most high-performance thermoset resins. Therefore, thermal degradation during the welding process of the thermoset resin in the TSC adherend as well as its connection with the coupling layer is a matter of concern. Possible strategies to avoid or minimise thermal degradation during high-temperature welding have been presented in the literature. One of them, experimentally assessed by Schieler et al [4], entails increasing the thickness of the coupling layer, which can as well be regarded as a thermal shield. In their work they showed that a minimum PEI coupling layer thickness of 250 µm was required to successfully induction weld carbon/epoxy (RTM6) adherends to carbon/PEI adherends at a welding temperature of 300°C. Another strategy, introduced in our previous work [10] entails using very fast heating rates and hence very short welding times (typically under 0.5 s), as for instance enabled by ultrasonic welding, to prevent the occurrence of any significant degradation reactions even in the absence of the thermal shield provided by the coupling layer [11].

The experimental study presented in this paper aimed at investigating ultrasonic welding of carbon/epoxy to carbon/PEEK composites through a PEI coupling layer. It builds on results presented at the CANCOM (Canadian International Conference on Composite Materials) Conference in July 17-20 2017 Ottawa (Canada). Based on existing knowledge [5,8,9], the PEI coupling layer was expected to form a gradient interphase with a gradient morphology with the epoxy resin during the co-curing process used to obtain the weldable carbon/epoxy adherends.

Furthermore, based on the existence of total miscibility of PEI and PEEK above the melting temperature of the latter [13], the welding process was expected to result in molecular inter-diffusion between the PEI coupling layer and the carbon/PEEK adherend generating a local, high-performance PEI-PEEK blend. Finally, the use of ultrasonic welding was expected to either prevent or minimise thermal degradation during welding. The main following aspects were investigated in this experimental paper: morphology of the gradient interphase between epoxy and PEI, effect of the welding process on the gradient interphase and on the epoxy-based adherends, and strength of the welded joints relative to reference joints. Finally, additional results of a side study on the use of a PEEK coupling layer to weld the same carbon/epoxy and carbon/PEEK material combination were presented.

2. Experimental

2.1 Materials and manufacturing of composite laminates

The thermoset composite used in this study was carbon fibre reinforced epoxy (Hexply M18-1, Hexcel), hereafter referred to as C/Ep. Hexply M18-1 is an epoxy-amine resin which contains TGMDA (tetraglycidyl ether methane diphenyl aniline), and MBDA (4,4'-Methylenbis-(2,6-diethylanilin)), MBIMA(4,4'-Methylenbis-(2-isopropyl-6-methylanilin) and DDS (4,4'-Diaminodiphenylsulfone) as curing agents [9]. It also contains 20% PEI, which is an amorphous thermoplastic polymer with a glass transition temperature of 218°C [14], for toughening purposes. The PEI content in this resin system is within the critical content range, i.e. 10-20%, in epoxy-amine systems. A critical PEI content in an epoxy-amine system is known to result in a co-continuous phase separation morphology. This morphology is characterized by two continuous phases, a PEI-rich phase and an epoxy-rich phase, intertwined with each other [8]. M18-1 epoxy pre-preg with carbon fabric reinforcement (1/4 twill weave) and 43% vol. resin content was used to manufacture the C/Ep-PEI (i.e. C/Ep with a co-cured PEI layer) composite laminates through an

autoclave curing cycle. Eight pre-preg layers were laid-up in a $[0/90]_{4S}$ configuration and a 50 µm-thick PEI coupling layer (Ultem 1000, Sabic) was laid on top of the last pre-preg layer. The C/Ep-PEI stack was subsequently vacuum bagged and cured in an autoclave following a two-hour curing plateau at 180°C and 6 bar pressure. The thickness of the final C/Ep-PEI laminate was around 2 mm. An aluminium caul plate was used to ensure good surface finish on both sides of the laminate. It must be noted that the thickness of the PEI coupling layer, i.e. 50 µm, was much smaller than that suggested by Schieler et al. as the minimum thickness to prevent thermal degradation of the epoxy resin during their subsequent induction welding process, i.e. 250 µm [4]. Reducing the thickness of the coupling layer down to 50 µm was enabled by the use of ultrasonic welding and its ultra-short heating times [10]. Thinner coupling layers have the advantages of reduced weld line thickness and hence reduced secondary bending effects and reduction of extra weight added to the structure (in the assumption of the coupling layer covering a bigger area than the area to be welded for ease in manufacturing).

The thermoplastic composite used was carbon fibre reinforced poly-ether-ether-ketone (Cetex, Ten Cate Advanced Materials), hereafter referred to as C/PEEK. PEEK is a semicrystalline thermoplastic polymer with a glass transition temperature of 143°C and a melting temperature of 343°C. Carbon fabric reinforcement (5 harness satin weave) powder-impregnated with PEEK resin (50% vol.) was used to manufacture the C/PEEK laminates in a hot platen press. Six C/PEEK pre-preg layers were laid up in a $[0/90]_{3S}$ configuration for a nominal final thickness around 1.9 mm. The press consolidation cycle featured a consolidation temperature of 385°C, consolidation pressure of 10 bar and 20 min consolidation time.

2.2 Welding equipment and welding process

A Rinco Dynamic-3000 microprocessor-controlled ultrasonic welder operated at 20 kHz frequency and maximum power of 3 kW was used for this research. Composite adherends of

dimensions 25 mm x 100 mm were welded in a single lap configuration with an overlap length of 12.7 mm. These adherends were water-jet cut to the right dimensions from the C/Ep-PEI and the C/PEEK laminates. A custom-designed welding jig was used to ensure proper clamping and parallelism of the adherends throughout the welding process. A 40 mm-diameter titanium cylindrical sonotrode was used, which completely covered the 25 mm x 12.7 mm welding overlap. Figure 1 shows the ultrasonic welding setup.

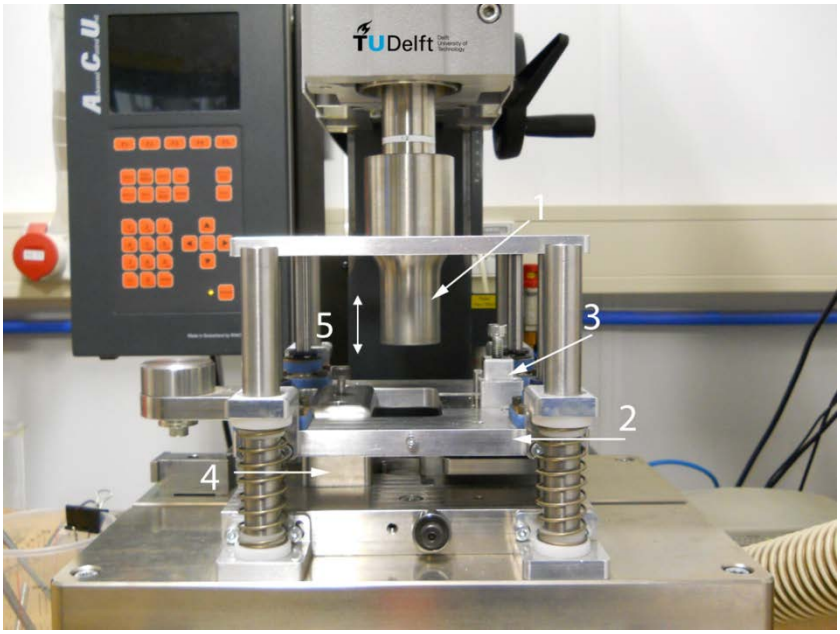

Figure 1. Ultrasonic welding setup: (1) sonotrode, (2) moving platform for top clamp, (3) top clamp, (4) bottom clamp, (5) direction of the vibration.

Two different types of welded joints involving thermoset composite were created in this study, namely (i) C/Ep-PEI welded to C/PEEK and (ii) C/Ep-PEI welded to C/Ep-PEI. Fully thermoplastic composite welded joints, i.e. C/PEEK welded to C/PEEK, were also manufactured as a reference joint for comparison purposes. A second type of reference joints, namely C/Ep to C/Ep joints obtained through a traditional co-curing autoclave process (same cycle as described in Section 2.1), were also analysed in this study. In order to ease the comparison between this second type of

reference joints and the welded joints, a 50 µm-thick PEI layer, i.e. same thickness as the coupling layer, was placed in between the two C/Ep pre-preg stacks prior to the co-curing process.

For all the above-mentioned welded joints a 250 µm-thick flat PEI (Ultem 1000) energy director was used to concentrate heat generation at the welding interface. Flat energy directors are neat resin films with an area slightly larger than the overlap which are placed between the adherends prior to the welding process and provide similar results to more traditional moulded energy directors [15]. The thickness of the PEI energy director was chosen based on our previous study on ultrasonic welding of C/PEI composites with different thickness PEI flat energy directors [16]. According to this study relatively thick energy directors, with thickness equal or higher than 250 µm, provide better results in terms of weld quality and process control than thinner energy directors. It must be noted, however, that during the welding process most of the molten energy director is squeezed out of the welding overlap, resulting in very thin weld lines (similar thickness as that of resin-rich regions within adherends in TPC to TPC welding [17]).

In the welding process the duration of the ultrasonic vibration was indirectly controlled by the downward displacement of the sonotrode under a constant welding force, normally referred to as displacement-controlled welding [17]. The optimum displacement for each material combination (i.e. displacement of the sonotrode that results in maximum lap shear strength) was graphically determined from the power and displacement data provided by the ultrasonic welder for calibration welds following the procedure explained in [17]. The different steps in the welding process were hence as follows: (1) A welding force of 2000 N and a 73.4 µm peak-to-peak vibration amplitude were applied until the optimal displacement was reached as a result of melting and squeeze out of the energy director; (2) Subsequently the vibration was stopped and a force of 1000 N was applied for 4 s to achieve consolidation of the welded joint during cooling. A combination of high welding force and high vibration amplitude were used in order to attain ultra-short heating times to prevent thermal degradation of the C/Ep material [10]. Table 1 lists all the different types of samples

considered in this study together with the optimum displacement values and the corresponding heating times.

Table 1. Different types of joints investigated in this research (*Reference joints). ED = energy director, WF= welding force, A=amplitude.

Joint reference	Optimum displacement (mm)	Average vibration time± stdev (ms)	Joining process
C/Ep-PEI-C/PEEK	0.16	421±48	Welding Flat ED (PEI, 250µm) WF= 2000 N A= 73.4 µm
C/Ep-PEI-C/Ep	0.16	479±57	
C/PEEK-C/PEEK*	0.22	550±37	
C/Ep-PEI-C/Ep*	-	-	Autoclave co-curing PEI interlayer

2.3 Testing and analysis

The welded and reference joints were mechanically tested following the ASTM D 1002 standard in a Zwick 250 kN universal test bench with a cross-head speed of 0.13 mm/min. Five coupons were tested per each type of joint and for every coupon the apparent lap shear strength was calculated as the maximum load divided by the overlap area.

Optical and scanning electron (SEM) cross sectional microscopy were used to investigate the internal structure of the adherends and of the welded joints. In order to resolve the microstructure of the Ep-PEI interphase the microscopy samples were etched with NMP (N-Methyl-2-pyrrolidone). The etching process entailed dripping 1 ml of NMP on the surface of the polished microscopy sample, followed by rinsing with ethanol and with distilled water and drying with compressed air. Additionally, Raman spectroscopy was used as a tool to help distinguish between PEI and epoxy molecules on a certain area of a cross section. Given the significant difference in response between PEI and the epoxy system used in this work at 1005 cm^{-1} wavelength in the Raman spectrum, that specific peak was used to create false colour plots to qualitatively identify areas with different PEI and epoxy content. For this purpose, a Renishaw inVia Raman microscope provided with a 785 nm and 200 mW laser was used. In the experiments 1% of the total available laser power was used to

irradiate the samples during 1 second per measurement. Sample preparation was done following the same procedure as for optical microscopy samples but no etching was required.

3. Results and discussion

3.1 Ep-PEI interphase in C/Ep-PEI laminate

PEI and most common epoxy resin systems are known to be compatible and to form a micron-size Ep-PEI gradient interphase with a gradient morphology. This results from local interdiffusion between epoxy and PEI while the former is in a liquid, reactive state. Subsequently, and owing to the generally limited solubility of PEI in cured epoxy systems, phase separation occurs once the epoxy resin reaches its gel point during curing [5,8,9]. To investigate the formation of a Ep-PEI interphase in the C/Ep-PEI laminate produced in this study, cross section analysis was performed on samples obtained from the laminate with the following results.

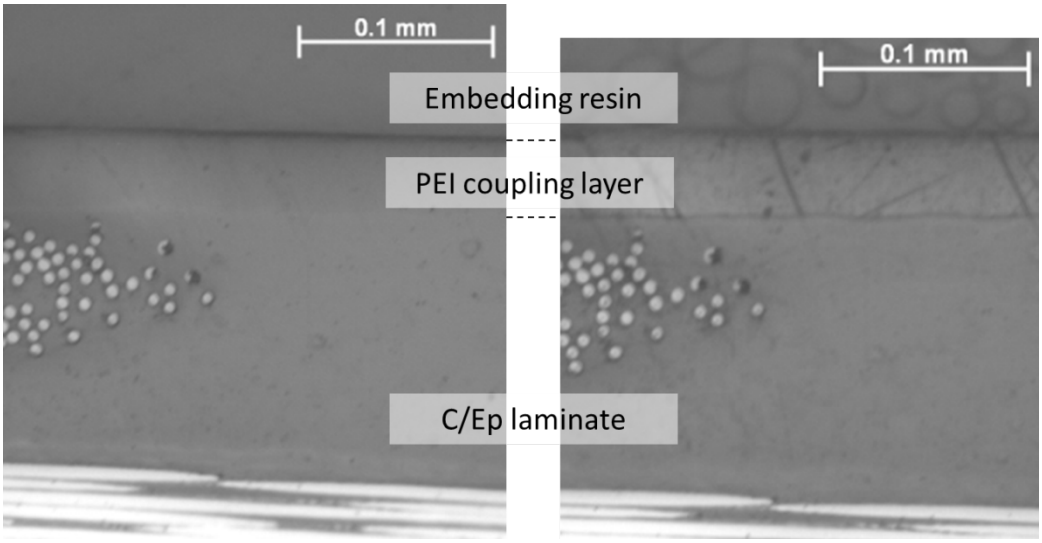

Figure 2. Cross section optical micrographs of C/Ep-PEI laminate: before etching (left) and after NMP etching (right)

Optical microscopy of non-etched samples did not show any significant differences in appearance between the PEI and epoxy resins (Figure 2). Optical microscopy of etched samples allowed differentiation between the PEI layer and the epoxy resin but showed a distinct line

separating the PEI layer and the C/Ep composite instead of a wider band corresponding to the expected interphase region (Figure 2). It should be noted that, according to the literature, the interphase thickness for different PEI-epoxy systems under various curing cycles ranges between 10 and 400 µm [5,8,9]. It is also interesting to mention that a scratch-like texture appeared on the PEI layer after the etching process.

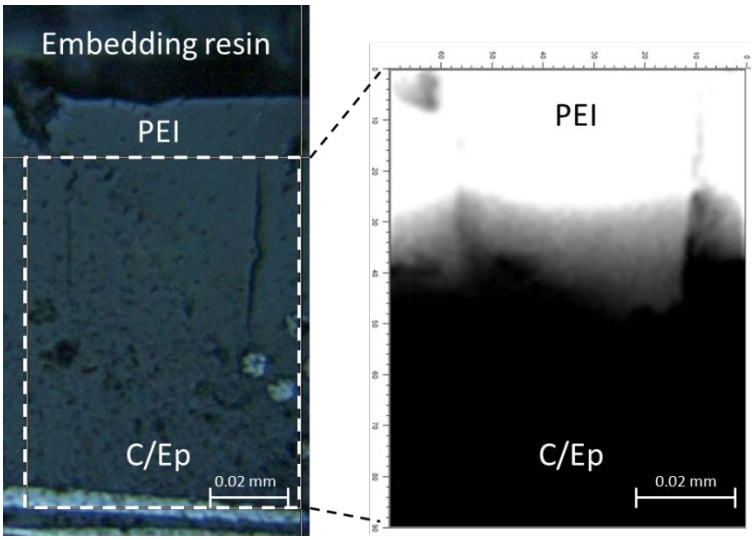

Figure 3. False colour plot (right) obtained from Raman spectroscopy on cross-section of sample from C/Ep-PEI laminate (left). Dashed rectangle on micrograph indicates area analysed. False colour plot is based on peak intensity at 1005 cm^{-1} wavelength. Black colour indicates 100% Ep and white colour indicates 100% PEI.

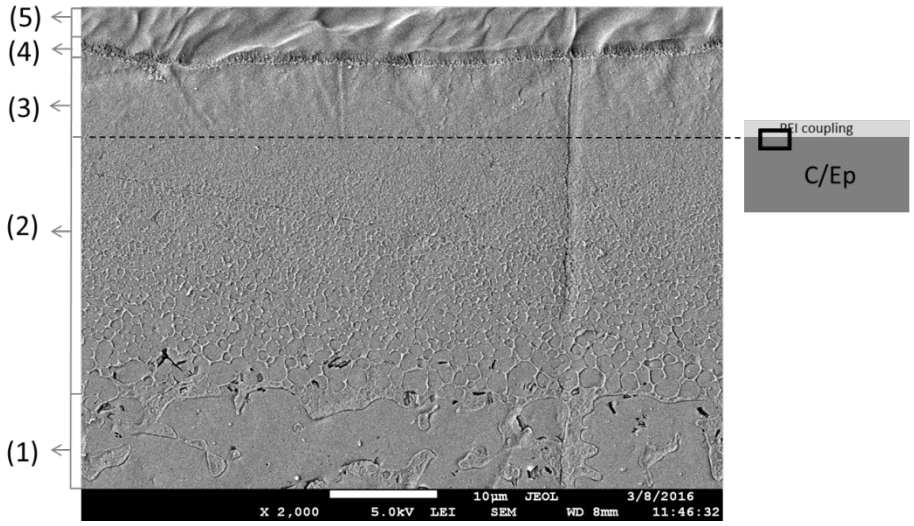

Figure 4. SEM image of the Ep-PEI interphase for NMP etched sample. The dotted line indicates approximate location of Ep-PEI boundary prior to the co-curing process. Numbers in between brackets indicate different regions. Approximate thickness of region (1) is 2 mm (only partially shown in the Figure), region (2) is 20 µm, regions (3) and (4) is 10 µm and region (5) is 40 µm (only partially shown in the Figure). Schematic on the left indicates approximate location of micrograph in C/Ep-PEI sample.

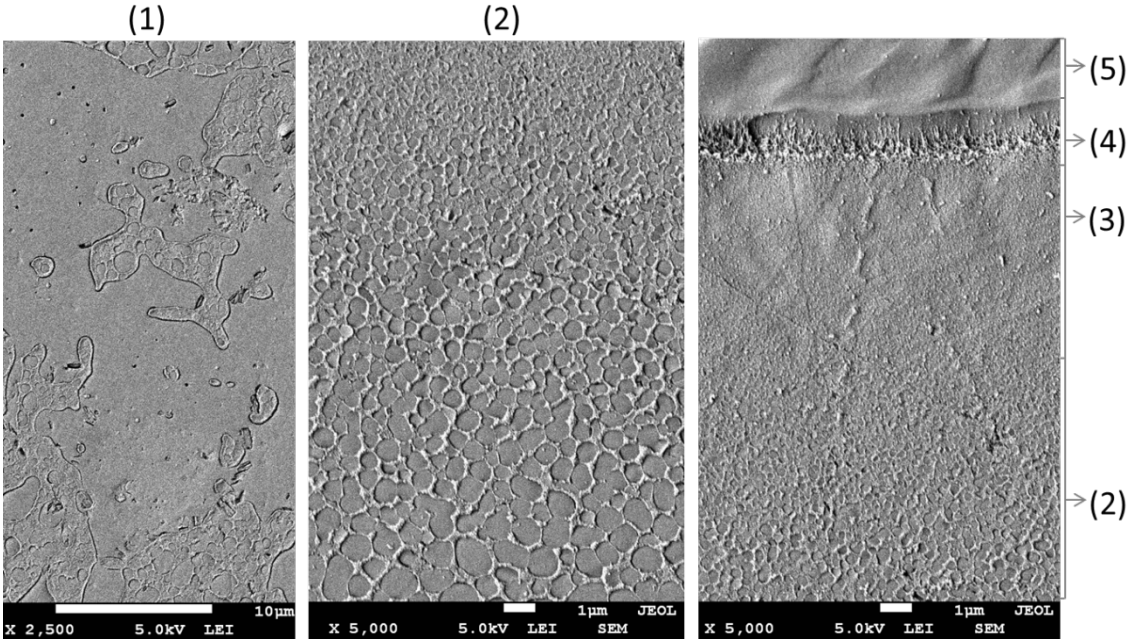

Figure 5. Details of morphologies in different regions (numbers in between brackets) in C/Ep-PEI SEM micrograph (NMP etched sample).

Contrarily, analysis of the cross section under Raman spectroscopy (Figure 3) in a false colour plot did show the existence of an in-between grey region with a composition between 100% PEI

(represented as white) and 100% original Ep resin (represented as black). Furthermore, SEM inspection of etched samples revealed the existence of different morphologies in the C/Ep-PEI cross section, as shown in Figures 4 and 5. According to these different morphologies, the C/Ep-PEI cross section was divided in the five different regions indicated in Figure 4. These were:

- Region 1: Co-continuous morphology, i.e. a phase-separation morphology composed of two continuous phases, one inside of the other, typical of toughened epoxy-amine systems with critical PEI content as explained in Section 2.1. This co-continuous morphology was found across the entire C/Ep-PEI cross-section, except for regions 2 to 5, as described in what follows.
- Region 2: Morphology characterised by epoxy spheres dispersed in a continuous PEI matrix typical of PEI toughened epoxy-amine systems with PEI content above the critical range [5,8]. The size of the epoxy spheres decreased when moving towards the pure PEI layer (region 5).
- Region 3: Region with very small dispersed epoxy spheres which also showed a light scratch-like texture which resembled the heavier scratch-like texture found in the pure PEI layer (region 5).
- Region 4: Relatively narrow band delimited by a front of small spheres on its lowest side (boundary with region 3) and a softer wave-like boundary on its top side (boundary with region 5). The sphere concentration decreased gradually between these two boundaries.
- Region 5: Pure PEI characterised by a heavy scratch-like texture caused by etching as observed in Figure 2.

Based on existing knowledge on Ep-PEI interphases, the formation of the regions described above can be explained as follows. In the early stages of the curing cycle, the reactive epoxy monomers started to diffuse into the glassy PEI layer through the original interface between the two

materials. The increasing content of epoxy monomers in the PEI resin led to swelling, glass-to-rubber transition and finally local dissolution of the PEI. The dissolved PEI polymers could then diffuse into the liquid epoxy locally increasing the content of PEI in the epoxy system above the initial 20%. Subsequent gelation of the epoxy later into the curing cycle stopped this interdiffusion process and caused phase separation between PEI and epoxy [8]. Considering the location of the original interface between the C/Ep composite and the PEI coupling layer, indicated by a dotted line in Figure 4, regions 3 and 4 resulted from the diffusion of the epoxy monomers into the PEI film. Of these, region 4 is believed to correspond to the epoxy penetration front. In this particular case, the penetration front showed two distinct boundaries. These two boundaries could probably have been caused by potentially different diffusion rates of the different monomers of the epoxy system (TGMDA, MBDA, MBIMA, DDS) in PEI [8]. On the other hand, region 2 resulted from the diffusion of the dissolved PEI into the liquid epoxy which increased the PEI content in the epoxy system above the original value. Upon gelation, phase-separation resulted in a morphology consisting of epoxy spheres in a continuous PEI matrix, characteristic of systems with PEI content above the critical range [8]. The decreasing size of the epoxy spheres when moving upwards in region 2 and into region 3, as well as the scratch-like texture in region 3, indicated decreased epoxy content, or in other words, increased PEI content, which is consistent with the composition of a typical solvent (i.e. un-cured epoxy)-polymer diffusion zone [8].

As clearly shown in Figure 3 and also seen during SEM analysis, the thickness of the Ep-PEI interphase was not uniform and seemed to be influenced by the presence of the fibre bundles, which are thought to act as a physical barrier to the diffusion process. The minimum thickness measured for the total interphase, defined as regions 2, 3 and 4, on the SEM cross sections was 30 μm. Approximately 2/3 of this total thickness corresponded to region 2 (i.e. PEI diffused into epoxy) and the remaining 1/3 to regions 3 and 4 (i.e. epoxy diffused into PEI). It should be noted that this interphase was 10 times thinner than the one formed between PEI and A-stage DGEBA-MCDEA

epoxy (DDS curing agent) as reported in literature [8]. Possible reasons for this discrepancy could be a lower diffusion speed of the B-stage epoxy present in the pre-preg used in this study, lower diffusion speed caused by the presence of PEI as a toughening element in the original epoxy resin, and finally the fibre reinforcement acting as a physical barrier to the diffusion of PEI, as mentioned before.

3.2 Welded joints

Despite the fact that the PEI coupling layer was much thinner than that used in a previous similar study, i.e. 50 µm in the present study versus 250 µm used by Schieler et al. [4], no visible signs of thermal degradation, i.e. porosity caused by resin sublimation, could be found in the C/Ep adherends after welding. As an example of the evidence used to support the latter statement, Figure 6 shows a representative cross section micrograph of a C/Ep-PEI-C/PEEK welded joint. Apart from lack of porosity in the C/Ep adherend, Figure 6 shows that the thickness of the PEI-rich area in between the C/Ep and the C/PEEK adherends, originally amounting to approximately 300 µm, i.e. coupling layer plus energy director, was reduced to approximately 100 µm during the welding process. Most of this thickness reduction was attributed to squeeze flow of the molten energy director out of the welding overlap although, as explained later, evidence of flow within the coupling layer was occasionally found. Regarding the post-welded Ep-PEI interphase, SEM observation indicated that the interphase was either unaffected (see Figure 7) or only slightly affected by the welding process. The way in which the welding process majorly affected the interphase was by displacing its outermost regions (mostly region 4, and less frequently region 3) through local melting and squeeze flow of the PEI coupling layer together with the energy director. As an example, Figure 8 shows an area of a C/Ep-PEI-C/PEEK welded overlap where both regions 3 and 4 were displaced by the squeeze flow taking place during welding.

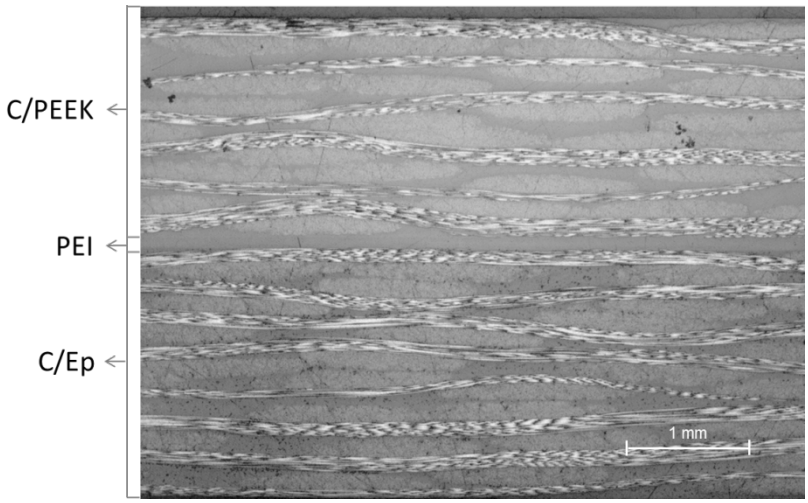

Figure 6. Cross section optical micrograph of C/Ep-PEI-C/PEEK welded sample before etching showing absence of porosity in C/Ep adherend. Note that the thickness of the PEI-rich weld-line is approximately 100 µm after squeeze out of the energy director during the welding process.

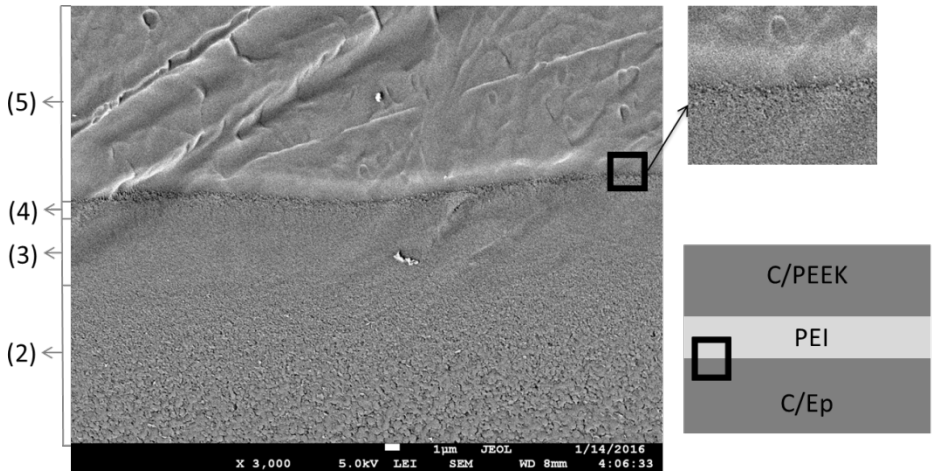

Figure 7. SEM image of post-welded interphase in C/Ep-PEI-C/PEEK welded and NMP etched sample. All regions in the C/Ep interphase are intact after the welding process. Schematic shows approximate location of micrograph.

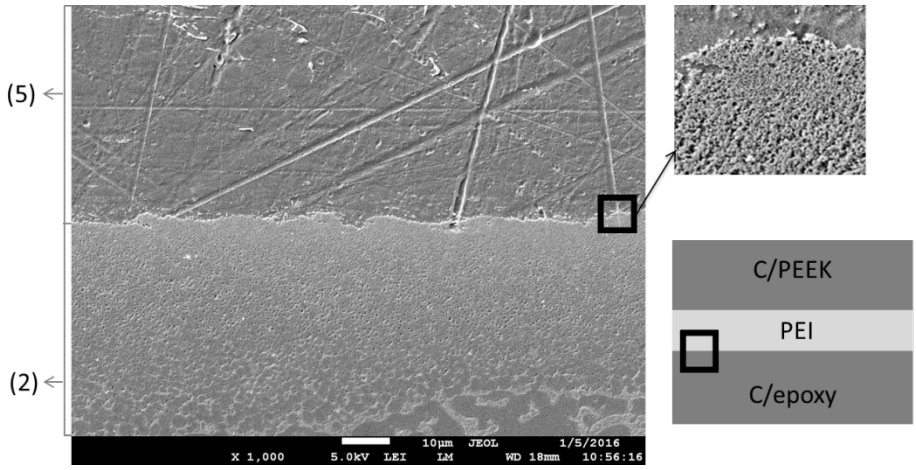

Figure 8. SEM image of post-welded interphase in C/Ep-PEI-C/PEEK welded and NMP etched sample. Regions (3), (4) and (5) have been displaced by melting and flow of the PEI coupling layer during welding.

Table 2. Apparent lap shear strength values for welded and reference joints (*).

Joint reference	**LSS (MPa)**	**Standard deviation (MPa)**	**Notes**
C/Ep-PEI-C/PEEK	28.6	2.3	Welded joint
C/Ep-PEI-C/Ep	23.6	0.9	Welded joint
C/Ep-PEI-C/Ep*	26.5	0.7	Co-cured in autoclave
C/PEEK-C/PEEK*	42.4	4.5	Welded

Mechanical testing of the welded joints provided the apparent lap shear strength (LSS) values listed in Table 2. The C/Ep-PEI-C/PEEK welded joints resulted in an average 28.6 MPa LSS with 8% scatter (coefficient of variation). The C/Ep-PEI-C/Ep welded joints resulted in a somewhat lower average LSS, amounting to 23.6 MPa with 4% scatter. Both types of joints showed cohesive failure in the C/Ep adherend as the main failure mechanism. SEM inspection of the cross section of fractured samples seemed to indicate that failure did not preferentially occur at the Ep-PEI interphase but within the C/Ep material itself (see Figure 9). Further research is however needed for in-depth characterisation the fracture surfaces and the locus of failure in these welded joints. It is however interesting to mention that both types of welded joints showed unwelded areas towards the

middle of the overlap. These unwelded areas were characterized by smooth and shiny mating fracture surfaces, consistent with adhesive failure at the welding interface. They were believed to result from the combination of short heating times and the relatively lower temperatures in the middle of the overlap [18], which locally hindered molecular interdiffusion across the welding interface. In the case of the C/Ep-PEI-C/PEEK welded joints the unwelded areas amounted to 25% of the total overlap. In the case of the C/EP-PEI-C/Ep welded joints, they covered approximately 5% of the total overlap. The bigger unwelded areas in the C/Ep-PEI-PEEK welds were attributed to the fact that, in order for molecular interdiffusion to occur at the PEI-PEEK welding interface, the melting temperature of PEEK needed to be reached. The melting temperature of PEEK is however significantly higher that the temperature at which the PEI energy director would soften and start to flow (i.e. above its glass transition temperature). Further optimisation of the welding process by, for instance, adequately modifying the energy director to minimise these unwelded areas will be addressed in further research. Despite having bigger unwelded areas the C/Ep-PEI-C/PEEK welded joints showed somewhat higher LSS than the C/Ep-PEI-C/Ep welded joints . This could have resulted from (i) potential differences in the stiffness between the C/Ep and C/PEEK adherends or (ii) differences in the thickness of the PEI-rich area between the adherends (thicker PEI-rich area in the C/Ep-PEI-C/Ep joints owing to the presence of two coupling layers). Both factors are known to influence the stresses at the weld line and hence the results of the lap shear test [19].

As also shown in Table 2, the LSS provided by the C/Ep-PEI-C/Ep co-cured reference samples (26.5 MPa, 3% scatter) was close to the LSS of the corresponding welded joints. The failure observed in these reference samples was cohesive within the C/Ep adherends. Further research is however necessary to discern whether failure predominantly occurred within the C/Ep material itself or within the Ep-PEI interphase. The similarities between strength and failure in the co-cured and the welded C/Ep-PEI-C/Ep joints once more indicated that the welding process did not significantly damage the strength of the C/Ep adherends or that of the Ep-PEI interphase. The

somewhat lower LSS of the welded joints was attributed to (i) the presence of unwelded areas in the overlap and/or (ii) the thickness difference between the PEI-rich area between the two C/Ep adherends (approximately 100 μm thicker in the case of the welded joints). Finally, the LSS provided by the C/PEKK-C/PEEK welded joints was 43 MPa with 10% scatter, featuring predominant cohesive failure in the first ply of the C/PEEK adherends and unwelded areas amounting to 20-25% of the total overlap. The fact that the LSS of the C/PEEK-C/PEEK welds was significantly higher than the one provided by the C/Ep-PEI-C/PEEK joints could be attributed to (i) different stresses at the weld line and (ii) the higher ductility of the C/PEEK composite and hence more energy consumed during failure. It should be noted that owing to the complex stress state at the overlap during single lap shear testing [18], direct comparison of the LSS values of the welded joints with interlaminar strength of the composite adherends is not a straightforward task. For this reasons, single lap shear reference samples were considered to be more meaningful in this study.

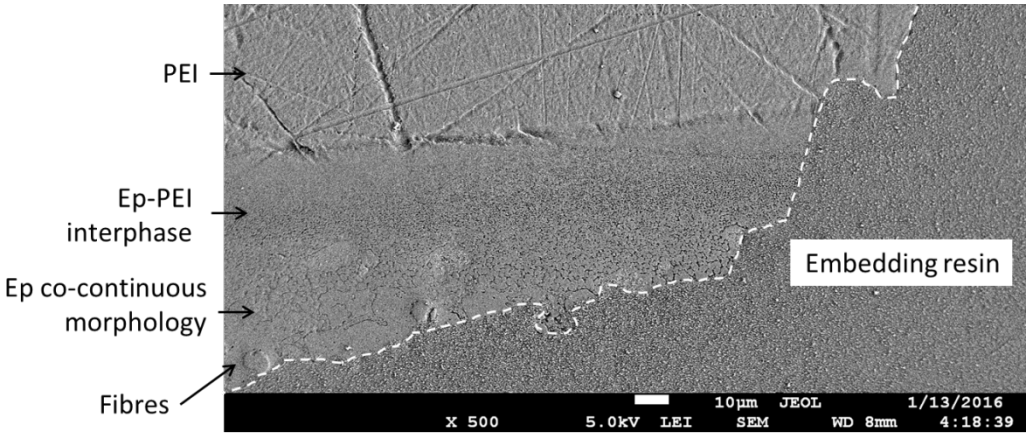

Figure 9. SEM image of a crack path in a C/Ep-PEI-C/PEEK welded and NMP etched sample (white dashed line).

3.3 PEEK as coupling layer material (side study)

Additional experiments were carried out to explore the use of PEEK as an alternative coupling layer material [7,10] for the dissimilar composite welded joints considered in this study. Similarly to the case of the PEI coupling layer discussed in this paper, the PEEK coupling layer (Victrex,

grade 1000) had a thickness of 50 μm and it was co-cured with the C/Ep pre-preg stack following the procedure explained in Section 2.1. Owing to its high chemical resistance, PEEK is generally not soluble in un-cured epoxy systems. Consequently the PEEK coupling layer was subjected to UV-O_3 treatment for 30 min prior to lamination in order to promote its adhesion with the epoxy resin [7,10] after unsuccessful attempts to work with an untreated PEEK coupling layer. After the co-curing process, a weldable C/Ep-PEEK laminate was obtained. Figure 10 shows a SEM cross-section of an etched sample obtained from this laminate. In this micrograph there is a clear cut between the epoxy resin, with its original co-continuous morphology (as seen in Figures 4 and 5), and the PEEK resin. As expected, no gradient morphologies could be observed in the C/Ep-PEEK laminate.

Adherends cut from the C/Ep-PEEK laminate were welded to C/PEEK adherends following the procedure described in Section 2.2. In this case, however, a PEEK energy director was used (flat energy director of 250 μm thickness from Victrex, grade 1000). The optimum sonotrode displacement during the welding process was set to 0.16 mm, which led to an average heating time of 516 ms. As in the case of the C/Ep-PEI-C/PEEK welded joints, the C/Ep-PEEK-C/PEEK joints did not show any visible signs of thermal degradation during the welding process. Figure 11 shows absence of voids in a C/Ep-PEEK-C/PEEK welded sample. It also shows that, similarly to the case of the C/Ep-PEI-C/PEEK welded joints (see Figure 6), the final thickness of the PEEK-rich area in between the adherends was approximately 100 μm.

The average lap shear strength of these C/Ep-PEEK-C/PEEK welded joints was very similar to those of the C/Ep-PEI-C/PEEK welded joints discussed before, namely 29.9 MPa (9% scatter) for the former versus 28.6 MPa (8% scatter) for the latter. Likewise, cohesive failure within the C/Ep adherend was the predominant failure mode in both types of joints, with unwelded areas which amounted to 5% of the total overlap area. Moreover, immersion of the welded joints in water at 70°C for one week did not cause any measurable drop on the LSS or change in the location of

failure in any of these joints, contrarily to initial expectations according to which such conditioning might damage the connection between C/Ep and the PEEK coupling layer. However a drastic loss in the adhesion of the PEEK coupling layer was observed approximately three months after the manufacturing of the C/Ep-PEEK laminate in leftover samples stored in the lab in standard conditions. The PEEK coupling layer spontaneously detached itself from the C/Ep composite at the edges of the samples and could be easily peeled off by hand. Contrarily, the leftover C/Ep-PEI samples, stored in the same conditions, did not show any visible indication of loss of adhesion even one year after their manufacture. These findings suggest that closer attention should be payed to understanding the long-term environmental resistance of the connection between the thermoplastic coupling layer and the thermoset substrate in weldable thermoset composites, especially on those cases where no interphase exists between the thermoplastic and thermoset materials. Moreover, owing to the amorphous nature of PEI, and hence a reduced chemical resistance as compared to semi-crystalline thermoplastic polymers such as PEEK, chemical resistance of the C/Ep-PEI-based welded joints should be further investigated as well.

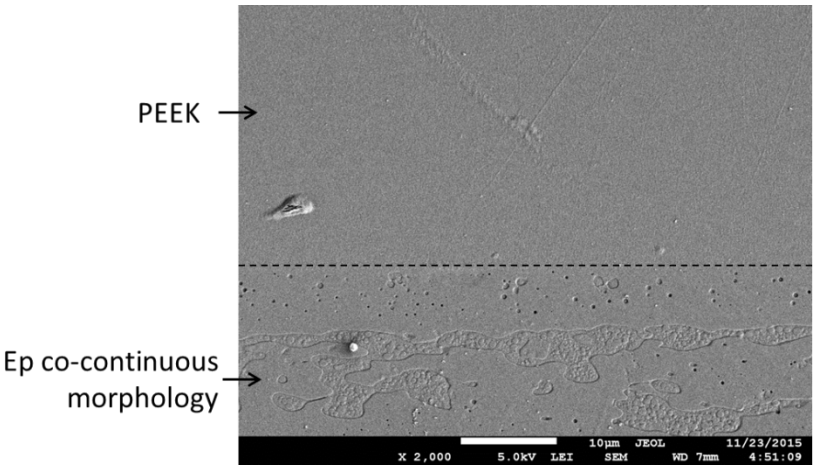

Figure 10. Cross-section SEM micrograph of etched sample obtained from C/Ep-PEEK laminate after co-curing process. Dashed line shows approximate location of interface between C/Ep and PEEK.

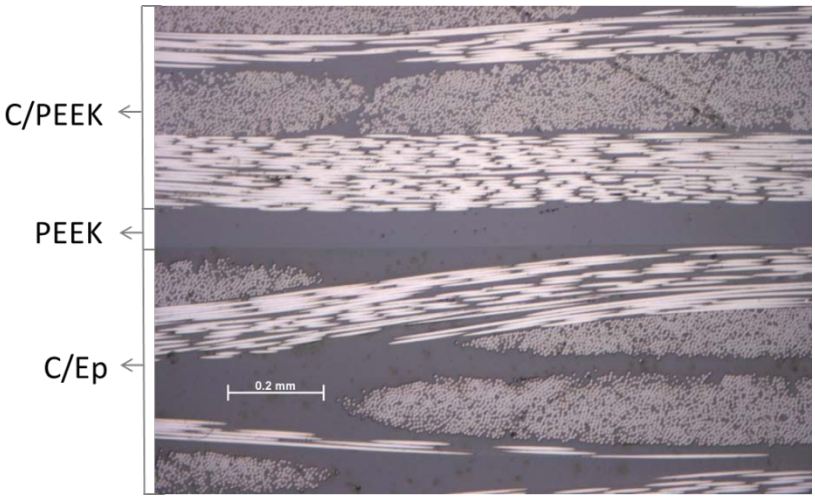

Figure 11. Cross-section optical micrograph of C/Ep-PEEK-C/PEEK welded sample showing no visible signs of thermal degradation (i.e. porosity) in the C/Ep adherend. Note that the thickness of the PEEK-rich weld-line is approximately 100 µm after squeeze out of the energy director during the welding process.

4. Conclusions

This paper presents research on welding of dissimilar composites, i.e. carbon/epoxy (C/Ep) and carbon poly-ether-ether-ketone (C/PEEK) composites. The main features of the welding procedure are: (i) a 50 µm-thick PEI film was used as a coupling layer to obtain weldable C/Ep laminates in which the epoxy matrix gradually evolved into the PEI thermoplastic polymer on the surface to be welded through a gradient interphase which featured a gradient morphology, (ii) the C/Ep-PEI adherends were welded to the C/PEEK adherends exploiting the full miscibility between PEI and PEEK above the melting temperature of the latter and (iii) ultrasonic welding was used to enable high-temperature welding without thermal degradation of the C/Ep material. The main conclusions drawn from this research are as follows:

- Co-curing of a PEI film on the welding surface of the C/Ep laminates used in this study resulted in a gradient interphase in which the original PEI content in the PEI-toughened epoxy resin gradually increased until pure PEI was obtained on the surface. This gradual

increase of PEI content could be qualitatively assessed through morphological changes in the resin revealed by SEM inspection of etched samples. On one hand, partial diffusion of the PEI film into the epoxy resin caused the original co-continuous morphology in the epoxy resin to evolve into a PEI-richer morphology consisting of epoxy spheres dispersed in PEI matrix. The size of these epoxy spheres gradually decreased as the PEI content increased towards the surface. On the other hand, diffusion of the epoxy monomers into the PEI film resulted in a distinct diffusion front within the PEI coupling layer.

- The Ep-PEI interphase had a minimum total thickness of 30 μm and it was mostly found between the outermost layer of reinforcing fibres in the C/Ep composite and the PEI coupling layer. Of this thickness, approximately 2/3 corresponded to the area where PEI diffused into the epoxy resin and the other 1/3 to the area where epoxy diffused into the PEI layer.
- Owing to melting and local flow of the PEI coupling layer during the welding process, the area of the interphase corresponding to epoxy diffusion into the PEI coupling layer, i.e. the outermost regions of the interphase, was found to disappear in some areas of the welding overlap. However, the rest of the interphase as well as the C/Ep composite were not visibly affected by the welding process.
- The average lap shear strength provided by the C/Ep-PEI-C/PEEK welded samples was 28.6 MPa, with predominant cohesive failure within the C/Ep adherend. This strength value is comparable to strength values reported for high-performance adhesives and hence shows the potential of the proposed approach. In future research the welding process should however be optimised to prevent the occurrence of unwelded areas within the overlap.
- When the same welding process was applied to weld two C/Ep adherends the resulting average single lap shear strength was 24.8 MPa, which is quite similar to the 26.5 MPa

provided by reference C/Ep co-cured joints. Likewise, both types of joints primarily failed within the C/Ep adherends. These observations indicated that, apart from not causing any significant visible damage, the welding process did not significantly damage the mechanical properties of the C/Ep adherends or of the Ep-PEI interphase.

- Alternative C/Ep-PEEK-C/PEEK welded joints created by co-curing a UV-O_3 treated PEEK film with a C/Ep laminate showed similar as-manufactured single lap shear strength as the C/Ep-PEI-C/PEEK welded joints. However, after being stored in standard lab conditions for three months, the PEEK coupling layer was found to spontaneously peel off from the C/Ep composite. Even though the PEI coupling layer did not detach from the C/Ep composite, long-term performance, environmental and chemical resistance of dissimilar composite welded joints should be further investigated.

5. References

1. Offringa A, Myers D, Buitenhuis A. Redesigned A340-500/600 fixed wing leading edge (J-nose) in thermoplastics. In: Proceedings of the 22nd International SAMPE Europe Conference. Paris, April, 2001. p.331-43.
2. van Ingen JW, Buitenhuis A, van Wijngaarden M., Simmons F. Development of the Gulfstream G650 induction welded thermoplastic elevators and rudder. In Proceedings of the International SAMPE Symposium and Exhibition. Seattle, WA, 2010.
3. Deng S, Djukicb L, Paton R and Yea L. Thermoplastic epoxy interactions and their potential applications in joining composite structures: a review. Composites Part A: Applied Science and Manufacturing 2015; 68:121-132.
4. Schieler O., Beier U. Induction welding of hybrid thermoplastic-thermoset composite parts. KMUTNB: International Journal of Applied Science and Technology 2016; 9: 27-36.

5. Vandi LJ, Hou M, Veidt M, Truss R, Heitzmann M, Paton R. Interface diffusion and morphology of aerospace grade epoxy co-cured with thermoplastic polymers. In: Proceedings of the 28th Congress of the International Council of the Aeronautical Sciences, Brisbane, September 2012.
6. Jacaruso GJ, Davis GC, McIntire AJ. Method of making thermoplastic adhesive strip for bonding thermoset composite structures. United States Patent No. 5264059, 1993.
7. Shi H., Sinke J. Benedictus R. Surface modification of PEEK by UV irradiation for direct co-curing with carbon fibre reinforced epoxy prepregs. International Journal of Adhesion and Adhesives 2017; 73:51-57.
8. Lestriez B, Chapel J, Gerard J. Gradient interphase between reactive epoxy and glassy thermoplastic from dissolution process, reaction kinetics, and phase separation thermodynamics. Macromolecules 2001; 34(5):1204-1213.
9. Heitzmann MT, Hou M, Veidt M, Vandi LJ, Paton R.. Morphology of an interface between polyetherimide and epoxy prepreg. Advanced Materials Research 2011; 393-395:184-188.
10. Villegas IF, Vizcaino Rubio P. On avoiding thermal degradation during welding of high-performance thermoplastic composites to thermoset composites. Composites Part A: Applied Science and Manufacturing 2015; 77: 172-180.
11. Grefe H, Kreling S, van Moorlegehem R, Villegas IF, Dilger K. Fusion bonding of fiber reinforced thermoplastics and thermosets. In: Proceedings of the 17th European Conference on Composite Materials (ECCM17), Munich, June 2016.
12. Yousefpour A. Hojjati M., Immarigeon P. Fusion bonding/welding of thermoplastic composites. Journal of Thermoplastic Composite Materials 2014; 17:303-341.
13. Crevecoeur G, Groeninckx G. Binary blends of poly (ether ether ketone) and poly(ether imide), miscibility, crystallization behaviour and semicrystalline morphology. Macromolecules 1991; 24: 1190-1195.
14. ULTEM™ 1000B Natural Film: Product Data Sheet. Saudi Basic Industries Corporation (SABIC) 2017.

15. Villegas IF, Valle Grande B, Bersee HEN, Benedictus R. A comparative evaluation between flat and traditional energy directors for ultrasonic welding of CF/PPS thermoplastic composites. Composite Interfaces 2015; 22 (8): 717-729.
16. Palardy G., Villegas I.F. On the effect of flat energy director thickness on heat generation during ultrasonic welding of thermoplastic composites. Composite Interfaces 2017;24(2): 203-214.
17. Villegas IF. Strength development versus process data in ultrasonic welding of thermoplastic composites with flat energy directors and its application to the definition of optimum processing parameters. Composites Part A: Applied Science and Manufacturing 2014; 65: 27-37.
18. Levy A, Le Corre S, Villegas IF. Modelling of the heating phenomena in ultrasonic welding of thermoplastic composites with flat energy directors. Journal of Materials and Processing Technology 2014; 214: 1361-1371.
19. Guess TR, Allred RE, Gerstle FP. Comparison of lap shear test specimens. Journal of Testing Evaluation 1977; 5(3): 83-93.